

# An Artificial Frustrated System: Cold Atoms in 2D Triangular Optical Lattice

Yao-Hua Chen, Wei Wu, Hong-Shuai Tao, and Wu-Ming Liu  
*Beijing National Laboratory for Condensed Matter Physics,  
 Institute of Physics, Chinese Academy of Sciences, Beijing 100190, China*  
 (Dated: November 5, 2018)

We investigate the strongly correlated effect of cold atoms in triangular optical lattice by dynamical cluster approximation combining with continuous time quantum Monte Carlo method. When the interaction increases, Fermi surface evolves from a circular ring into a flat elliptical ring, system translates from Fermi liquid into Mott insulator. The transition between Fermi liquid and pseudogap shows a reentrant behavior due to Kondo effect. We give an experimental protocol to observe these phenomena by varying lattice depth and atomic interaction via Feshbach resonance in future experiments.

PACS numbers: 67.85.-d, 03.75.Hh, 03.75.Ss, 71.10.Fd

## I. INTRODUCTION

Quantum phase transition in strongly correlated system is an important research area in condensed matter physics, presenting some of the most challenging problems. In a real material, the experimental parameter is hard to be varied to observe the strongly correlated effect, which is complicated by impurities and multiple bands. However, a new developing technology called optical lattices presents a highly controllable and clean system for studying strongly correlated system, in which the relevant parameter can be adjusted independently [1–6]. Optical lattices with different geometrical property can be set up by adjusting the propagation directions of laser beams, such as triangular [7], honeycomb [8] and kagomé [9–12] optical lattice. The interaction between the trapped atoms is tunable through the Feshbach resonance, such as  ${}^6\text{Li}$  and  ${}^{40}\text{K}$ . In recent years, a series of experiments have been carried out to investigate the quantum phase transition of cold atoms in optical lattice [13–19].

There are many analytical and numerical methods to investigate the strongly correlated system, especially the frustrated system [20–29]. The dynamical mean-field theory (DMFT) [30] has been proved to be a useful tool. The self-energy is given as a local quantity in DMFT, which has been proved to be exact in the infinity dimensional limit [31]. This method is a good approximation even in three dimensional situation [32]. However, in the frustrated systems, the nonlocal correlations can not be simply ignored, DMFT would not work efficiently. So, many methods have been improved to incorporate nonlocal correlations in the framework of DMFT, such as dynamical cluster approximation (DCA) [33, 34]. Different with the DMFT, the lattice problem is mapped into a self-consistently embedded finite-sized cluster in DCA. The irreducible quantities of the embedded cluster is used as an approximation for the corresponding lattice quantities. DCA has been used to investigate the geometrical frustrated system [35, 36].

In present Letter, we investigate the Mott transition in an artificial frustrated system – cold atoms in triangu-

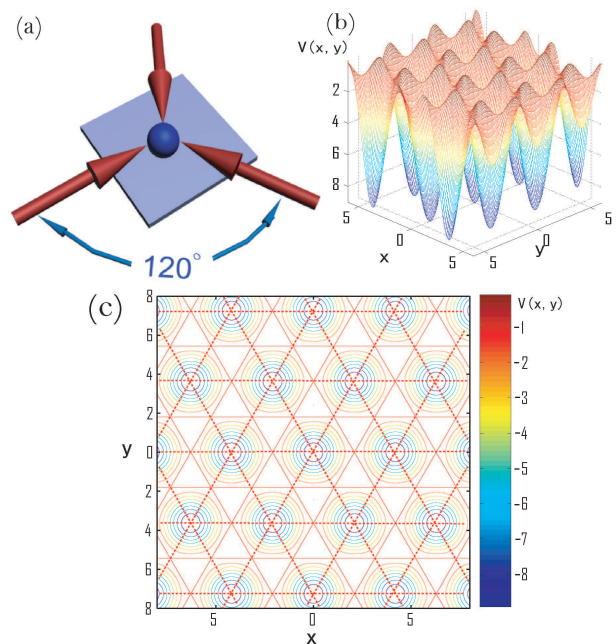


FIG. 1: (Color online) (a) Sketch of experimental setup to form triangular optical lattice. Each arrow depicts a laser beam, the sphere in center of the figure depicts the fermionic quantum gas, such as  ${}^{40}\text{K}$ . (b) Landscape of potential  $V(x, y)$ . (c) The contour lines of triangular optical lattice. The dark blue circles indicate the minimum lattice potential. The dash red lines show the geometry of this triangular optical lattice by connecting the minimum lattice potential.

lar optical lattice. We improve the numerical method – DCA combining with the continuous time quantum Monte Carlo method (CTQMC) [37] to investigate this geometrical frustrated system. CTQMC, used as the impurity solver, is an exact numerical method proposed recently. By calculating the density of states and the spectral function, we find the system undergoes a second order phase transition from Fermi liquid to Mott insulator. The phase diagram shows a reentrant behavior of the transition between Fermi liquid and pseudogap due to

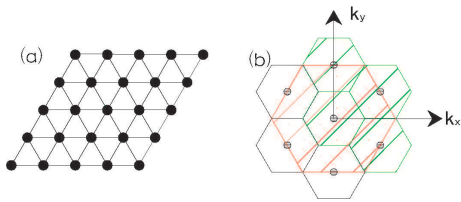


FIG. 2: (Color online)(a) Sketch of triangular lattice. (b) Coarse graining procedure in the first Brillouin Zone when  $N_c = 4$ . The red part shows the first Brillouin Zone in reciprocal space. The green part shows the region divided into 4 cells for DCA calculation.

the Kondo effect at low temperature. These phenomena can be observed in the triangular optical lattice by varying the lattice depth and the interaction strength via the Feshbach resonance. The advantage of this artificial frustrated system is highly controllable and cleanliness. And the numerical method acts as a powerful tool for investigating the strongly correlated effect in condensed matter physics, such as the spin liquid, the high-temperature superconductor and the colossal magnetoresistance.

## II. ARTIFICIAL FRUSTRATED SYSTEM

In contrast with real materials, the cold atoms trapped in an optical lattice provide an artificial system to investigate the strongly correlated effect. The experiment can be performed with  $^{40}\text{K}$  atoms prepared by mixing two magnetic sublevels of the  $F = 9/2$  hyperfine manifold, such as the  $|-9/2\rangle$  and the  $|-5/2\rangle$  states [16]. As an artificial frustrated system, the triangular optical lattice can be set up by three laser beams, such as the Yb fiber laser at wavelength  $\lambda = 1064$  nm, with a  $2\pi/3$  angle between each other, as illustrated in Fig. 1(a). The potential of optical lattice is given by

$$V(x, y) = V_0(3 + 4 \cos(\frac{k_x x}{2}) \cos(\frac{\sqrt{3}k_y y}{2}) + 2 \cos(\sqrt{3}k_y y)), \quad (1)$$

where  $V_0$  is the barrier height of standing wave formed by laser beams in the x-y plane,  $k_x$  and  $k_y$  are the two components of wave vector  $k = 2\pi/\lambda$  along x and y directions. In experiments,  $V_0$  is always given in units of recoil energy  $E_r = \hbar^2 k^2 / 2m$ . The landscape of potential of triangular optical lattice in the x-y plane is shown in Fig. 1(b), where the dark blue parts in the figure indicate the minimum lattice potential. Fig. 1(c) shows the contour lines of the triangular optical lattice. By connecting the center of the circular which indicates the minimum lattice potential, we may get the geometry of this triangular optical lattice, as shown by the red dash lines.

The Hamiltonian of the interacting fermionic atoms trapped in this artificial frustrated system is written as

$$H = -t \sum_{\langle ij \rangle \sigma} c_{i\sigma}^\dagger c_{j\sigma} + U \sum_i n_{i\uparrow} n_{i\downarrow}, \quad (2)$$

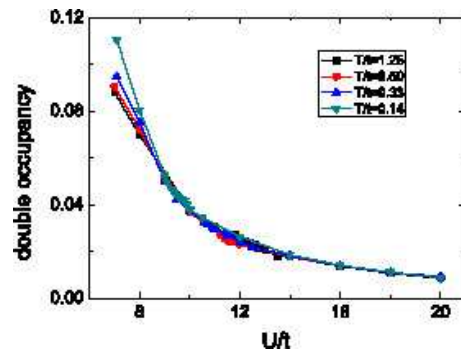


FIG. 3: (Color online) The double occupancy  $D_{occ}$  as a function of the interaction  $U$  for different temperature.  $t$  is the kinetic energy in equation (2).

where  $c_{i\sigma}^\dagger$  and  $c_{i\sigma}$  denote the creation and the annihilation operator of the fermionic atom on lattice site  $i$  respectively,  $n_{i\sigma} = c_{i\sigma}^\dagger c_{i\sigma}$  represents the density operator of fermionic atom. And  $t = (4/\sqrt{\pi})E_r(V_0/E_r)^{3/4} \exp(-2(V_0/E_r)^{1/2})$  is the kinetic energy, which can be adjusted by the lattice depth  $V_0$ .  $U = \sqrt{8/\pi}k a_s E_r(V_0/E_r)^{3/4}$  is the on-site interaction determined by the s-wave scattering length  $a_s$ , which can be adjusted by Feshbach resonance [6, 38, 39].

## III. NUMERICAL METHOD: DCA+CTQMC

We improve the dynamical cluster approximation (DCA) to combine with the continuous time Quantum Monte Carlo method (CTQMC) to investigate the strongly correlated effect of cold atoms in the frustrated system shown in Fig. 2(a), which can be realized by Hubbard model (2).

In DCA, the reciprocal space of the lattice containing  $N$  points is divided into finite cells [34]. The coarse-graining Green's function  $\bar{G}$  is achieved by averaging Green's function  $G$  within each cell. The lattice problem is mapped into a self-consistently embedded finite-sized cluster. The coarse graining procedure of the DCA is illustrated as follows: the Brillouin zone is divided into  $N_c$  cells, each cell is represented by a cluster momentum  $\vec{K}$ . In Fig. 2(b), we provide an example of this coarse graining procedure in  $N_c = 4$  situation. In our treatment, the coarse-grained Green's function

$$\begin{aligned} \bar{G}(\vec{K}, i\omega_n) &= \frac{N_c}{N} \sum_{\vec{k}} G(\vec{K} + \vec{k}, i\omega_n) \\ &= \frac{N_c}{N} \sum_{\vec{k}} \frac{1}{i\omega_n - \varepsilon_{\vec{K}+\vec{k}} - \bar{\Sigma}_\sigma(\vec{K}, i\omega_n)}, \end{aligned} \quad (3)$$

where summation over  $\vec{k}$  is taken within the coarse-graining cell, the  $\omega_n$  is the Matsubara frequency.

Similar with DMFT, after mapping the Hubbard model to an Anderson impurity problem, we introduce

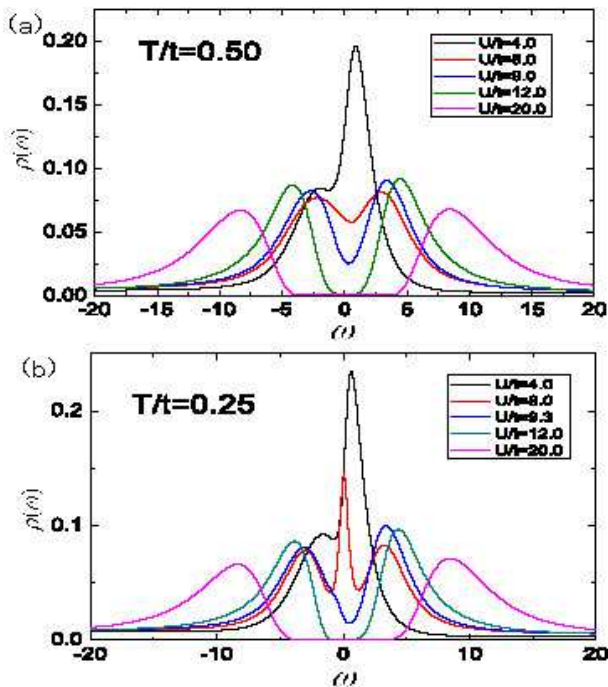


FIG. 4: (Color online) The density of states (DOS) as a function of frequency  $\omega$  for different interaction.  $t$  is the kinetic energy in equation (2). (a) At  $T/t = 0.50$ , a pseudogap formed by the splitting of Fermi-liquid-like peak appears when the interaction increases. A gap is opened when the interaction is stronger than the critical interaction  $U_c/t = 11.6$ . (b) At  $T/t = 0.25$ , a Kondo resonance peak is found before the pseudogap appears.

an impurity solver to solve the cluster problem, such as quantum Monte Carlo (QMC), fluctuation exchange approximate (FLEX), and the noncrossing approximation (NCA). In our calculation, we employ the CTQMC [37] which does not need to introduce any auxiliary-field variables as our impurity solver. Comparing with the traditional QMC method, the CTQMC is much more exact, because it does not use the Trotter decomposition. We use  $10^7$  sweeps in our CTQMC step.

The self-consist loop can be taken as follows:

1) The DCA iteration loop can be started by setting the initial self-energy  $\Sigma_c(\vec{\mathbf{K}}, i\omega_n)$  which can be guessed or be get from a perturbation theory.

2) We could get:

$$\overline{G}(\vec{\mathbf{K}}, i\omega_n) = \frac{Nc}{N} \sum_{\vec{\mathbf{k}}} 1/(i\omega_n - \varepsilon_{\vec{\mathbf{K}}+\vec{\mathbf{k}}} - \overline{\Sigma}_\sigma(\vec{\mathbf{K}}, i\omega_n)).$$

3) The host Green's function  $\overline{g}(\vec{\mathbf{K}}, i\omega_n)$  is computed by  $\overline{g}(\vec{\mathbf{K}}, i\omega_n)^{-1} = \overline{G}(\vec{\mathbf{K}}, i\omega_n)^{-1} + \Sigma_c(\vec{\mathbf{K}}, i\omega_n)$ .

4) The  $\overline{g}(\vec{\mathbf{K}}, i\omega_n)$  is transformed from momentum-frequency variable to space-time variable  $\overline{g}(\vec{\mathbf{X}}_i - \vec{\mathbf{X}}_j, \tau_i - \tau_j)$  used as the input to the CTQMC simulation.

5) The CTQMC step is the most time consuming part of the iteration loop. In our CTQMC step, we use  $10^7$  CTQMC sweeps. After the simulation, we get  $\overline{G}(\vec{\mathbf{X}}_i -$

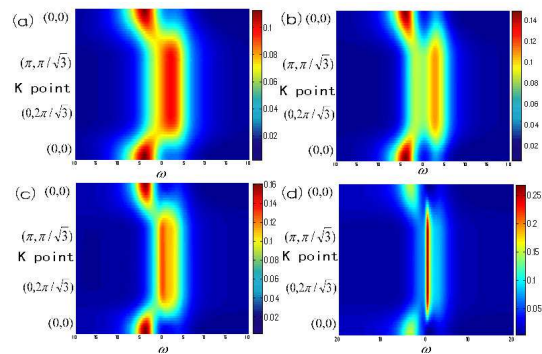


FIG. 5: (Color online) The K-dependent spectral function  $A_k(\omega)$  for different temperature, when  $U/t = 7.0$ .  $t$  is the kinetic energy in equation (2). (a) At  $T/t = 1.67$ , the red part shows a Fermi-liquid-like peak near Fermi energy. (b) At  $T/t = 1.11$ , a narrow pseudogap shown by green region. Two peak found around the pseudogap is shown by yellow and orange color. (c) At  $T/t = 0.5$ , a Fermi-liquid-like peak appears again shown by red color. (d) At  $T/t = 0.2$ , an obvious Kondo peak appears shown by red color.

$\vec{\mathbf{X}}_j, \tau_i - \tau_j)$ .

6)  $\overline{G}(\vec{\mathbf{X}}_i - \vec{\mathbf{X}}_j, \tau_i - \tau_j)$  is transformed from space-time variable to momentum-frequency variable  $\overline{G}(\vec{\mathbf{K}}, i\omega_n)$  by Fourier transform.

7) We get the new self-energy by  $\Sigma_c(\vec{\mathbf{K}}, i\omega_n) = \overline{g}(\vec{\mathbf{K}}, i\omega_n)^{-1} - \overline{G}(\vec{\mathbf{K}}, i\omega_n)^{-1}$ .

8) Repeat from step 2) to step 7) until  $\Sigma_c(\vec{\mathbf{K}}, i\omega_n)$  converges to desired accuracy.

9) Once convergence is reached, we can calculate the state density  $\rho(\omega)$  by maximum entropy method [40]. And we can get other lattice quantities by some other additional analysis code.

By combining the DCA, which introduces the nonlocal correlations, and the exact numerical method: CTQMC, we can investigate the frustrated system efficiently. This numerical method can be easily reconstructed to study another strong correlated system in the future research.

#### IV. PHASE DIAGRAM

We investigate the double occupancy  $D_{occ} = \partial F / \partial U = \frac{1}{4} \sum_i \langle n_{i\uparrow} n_{i\downarrow} \rangle$  as a function of interaction  $U$  for various temperature, where  $F$  is the free energy. When the interaction is lower than  $U/t = 8.6$ , the  $D_{occ}$  increases as the temperature decreases due to the enhancing of the itinerancy of atoms, as shown in Fig. 3. When the interaction is stronger than  $U/t = 8.6$ , the effect of the temperature on  $D_{occ}$  is weakened. The  $D_{occ}$  decreases as the interaction increases due to the suppressing of the itinerancy of the atoms. When the interaction is stronger than the critical interaction of the Mott transition,  $D_{occ}$  for different temperature is coincident, which shows the temperature does not affect the double occupancy dis-

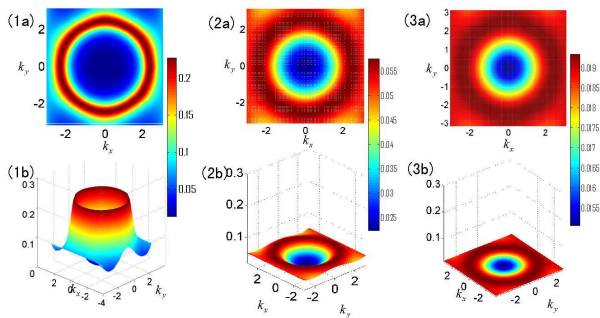


FIG. 6: (Color online) The Fermi surface as a function of momentum  $k$  for different interaction at  $T/t = 1.25$ : (1)  $U/t = 5.0$ , (2)  $U/t = 10.0$ , (3)  $U/t = 16.0$ .  $t$  is the kinetic energy in equation (2).

tinctly. The continuity of the evolution of the double occupancy by interaction shows that it is a second order transition.

We employ the maximum entropy method [40] to calculate the density of states (DOS) which describes the number of states at frequency  $\omega$ . Fig. 4(a) shows DOS for different interaction at  $T/t = 0.5$ . There is a Fermi-liquid-like peak when  $U/t = 4.0$ . A pseudogap formed by the splitting of Fermi-liquid-like peak appears when the interaction increases, such as  $U/t = 8.0$  and  $U/t = 9.0$ . When the interaction is stronger than the critical interaction  $U_c/t = 11.6$ , such as  $U/t = 12.0$  and  $U/t = 20.0$ , the system becomes an insulator indicated by an opened gap. DOS for different interaction at  $T/t = 0.25$  is shown in Fig. 4(b). When  $U/t = 4.0$ , there is also a Fermi-liquid-like peak. When the interaction increases, such as  $U/t = 8.0$ , a Kondo resonance peak appears which is shown by a sharp quasi-particle peak with two shoulders. When  $U/t = 9.3$ , the Kondo resonance peak is suppressed and a pseudogap appears, which is the intermediary state between the Fermi liquid and the Mott insulator. A gap is opened when the interaction is stronger than the critical interaction  $U_c/t = 10.6$ . Instead of directly splitting into two parts shown in Fig. 4(a), a Kondo peak appears, which is formed by the effect between the local atom and the itinerant atom at low temperature, as shown in Fig. 4(b).

We could also get the  $k$ -dependent spectral function  $A_k(\omega) = -ImG_k(\omega + i0)/\pi$ , which describes the distribution probability of the quasi-particle with momentum  $k$  and energy  $\omega$ . Fig. 5 shows  $A_k(\omega)$  for different temperature, where  $U/t = 7.0$ . At  $T/t = 1.67$ , there exists a quasi-particle peak which shows a metallic behavior, as shown in Fig. 5(a). In Fig. 5(b), a pseudogap appears at  $T/t = 1.11$ , which is formed by the splitting of the quasi-particle peak. When  $T/t = 0.50$ , the pseudogap disappears and there is a quasi-particle peak again, as shown in Fig. 5(c). An obvious Kondo peak appears when  $T/t = 0.2$ , as shown in Fig. 5(d). It shows a reentrant behavior in the transition between Fermi liquid and

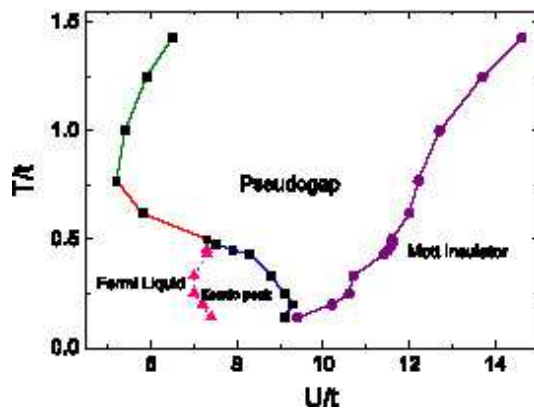


FIG. 7: (Color online) The phase diagram of Fermi atoms in triangular optical lattice, where the square plots with solid line (green, red, blue) indicate the transition line of the Fermi liquid and the pseudogap, the circular plots with solid line (purple) indicate the Mott transition line, the triangular plots with dash line (pink) mark the Kondo peak appearing region.  $t$  is the kinetic energy in equation (2).

pseudogap when the interaction is fixed and the temperature decreases. This behavior is based on the Kondo effect which suppresses the splitting of the quasi-particle peak at low temperature.

We study the Fermi surface as a function of momentum  $k$  by  $A(k; \omega = 0) \approx -\frac{1}{\pi} \lim_{\omega_n \rightarrow 0} ImG(k, i\omega_n)$ . A linear extrapolation of the first two Matsubara frequencies is used to estimate the self-energy to zero frequency [41]. Fig. 6 shows the Fermi surface for different interaction at  $T/t = 1.25$ . A circular ring which means the particles distribute on a certain energy displays a metallic behavior, as shown in Fig. 6(1a). As the interaction increases, the ring becomes bigger, as shown in Fig. 6(2a). When the interaction is stronger than the critical interaction  $U/t = 13.7$ , the Fermi surface becomes a nearly flat plane, as shown in Fig. 6(3a). From Fig. 6(1b) to Fig. 6(3b), we can find the amplitude of the spectral weight becomes small and the breadth become wider. The Fermi surface translates from a determined surface into a flat plane due to the localization of the particles when the interaction increases.

The phase diagram of cold atoms trapped in triangular optical lattice is shown in Fig. 7, where  $a_s$  indicates the  $s$ -wave scattering length. The translation between the Fermi liquid and the pseudogap shows a reentrant behavior. For a fixed interaction weaker than  $U/t = 7.2$ , when the temperature decreases, the system translates from Fermi liquid to pseudogap. When the temperature is lower than the critical temperature distributing on the red solid line, the system translates from pseudogap to Fermi liquid. There is a Kondo peak region, which is signed by the blue solid line and the pink dash line. If temperature is lower than  $T/t = 2.0$ , a Kondo peak emerges before the appearing of the pseudogap when the interaction increases. When the interaction is stronger than the critical interaction of Mott transition distribut-

ing on the purple line, the system translates from pseudogap to insulator confirmed by an opened gap.

## V. EXPERIMENTAL PROTOCOL

We design an experiment to investigate the quantum phase transition in triangular optical lattice. The experimental protocol can be taken as follows: The  $^{40}\text{K}$  atoms can be firstly produced to be a pure fermion condensate by evaporative cooling [42]. Three laser beams at wavelength  $\lambda = 1064$  nm are used to form the triangular optical lattice [43] to trap  $^{40}\text{K}$  atoms. The lattice depth  $V_0$  is used to adjust the kinetic energy  $t$  and the interaction  $U$ . The on-site interaction can be adjusted by Feshbach resonance [44–48]. The s-wave scattering length is used to determine the effective interaction. The temperature can be extracted from time-of-flight images by means of Fermi fits in experiment [19].

When the interaction increases, the system translates from Fermi liquid ( $a_s < 48a_0$ ) to Mott insulator ( $a_s > 111a_0$ ) at temperature  $T = 5.96nK$ , when  $V_0 = 10E_r$ . In order to detect the double occupancy  $D_{occ}$ , we increase the depth of optical lattice rapidly to prevent the further tunnelling first. Then, we shift the energy of atoms on doubly occupied sites by approaching a Feshbach resonance. And then, one spin component of atoms on the double occupied sites is transferred to a unpopulated magnetic sublevel by using a radio-frequency pulse. The double occupancy can be deduced by the fraction of transformed atoms obtained by the absorption imaging [16, 49]. At  $T = 5.96nK$ ,  $D_{occ}$  decreases from 0.11009 ( $a_s = 45a_0$ ) to 0.00456 ( $a_s = 130a_0$ ) with increasing atomic interaction.

By ramping down the optical lattice slowly enough, the atoms stay adiabatically in the lowest band while the quasi-momentum is approximately conserved. Then, the optical lattice is converted from a deep one into a shallow one and the quasi-momentum is preserved. After completely turning off the confining potential, the atoms ballistically expand for several milliseconds. Then by the absorption imaging, one can get the Fermi surface [50, 51]. At  $T = 5.96nK$ , the circular ring shape of the Fermi surface when  $a_s = 41a_0$  transforms into a flat plane when  $a_s = 162a_0$ .

## VI. SUMMARY

In summary, we investigate the Mott transition of the cold atoms in 2D triangular optical lattice set up by three laser beams. The system evolves from Fermi liquid into Mott insulator for increasing interaction, and a reentrant behavior of the transition between Fermi liquid and pseudogap is found, due to the Kondo effect. Our study presents a helpful step for understanding the strong correlated effect in the frustrated system, such as the spin liquid. Beyond DMFT, DCA is improved to incorporated the nonlocal correlation which can not be simply ignored in the frustrated system. This numerical method is universally to investigate strongly correlated system, such as the high-temperature superconductor and the colossal magnetoresistance.

This work was supported by NSFC under grants Nos. 10874235, 10934010, 60978019, the NKBRSCF under grants Nos. 2006CB921400, 2009CB930701 and 2010CB922904.

- 
- [1] D. Jaksch, C. Bruder, J. I. Cirac, C. W. Gardiner, and P. Zoller, *Phys. Rev. Lett.* **81**, 3108 (1998).
- [2] K. I. Petsas, A. B. Coates, and G. Grynberg, *Phys. Rev. A* **50**, 5173 (1994).
- [3] W. Hofstetter, J. I. Cirac, P. Zoller, E. Demler, and M. D. Lukin, *Phys. Rev. Lett.* **89**, 220407 (2002).
- [4] Y. Inada, M. Horikoshi, S. Nakajima, M. Kuwata-Gonokami, M. Ueda, and T. Mukaiyama, *Phys. Rev. Lett.* **101**, 180406 (2008).
- [5] M. Kottke, T. Schulte, L. Cacciapuoti, D. Hellweg, S. Drenkelforth, W. Ertmer, and J. J. Arlt, *Phys. Rev. A* **72**, 053631 (2005).
- [6] I. Bloch, J. Dalibard, and W. Zwerger, *Rev. Mod. Phys.* **80**, 885 (2008).
- [7] D. Jaksch, P. Zoller, *Ann. Phys. (N. Y.)* **315**, 52 (2005).
- [8] L. M. Duan, E. Demler, and M. D. Lukin, *Phys. Rev. Lett.* **91**, 090402 (2003).
- [9] L. Santos, M. A. Baranov, J. I. Cirac, H. U. Everts, H. Fehrmann, and M. Lewenstein, *Phys. Rev. Lett.* **93**, 030601 (2004).
- [10] B. Damski, H. Fehrmann, H. U. Everts, M. Baranov, L. Santos, and M. Lewenstein, *Phys. Rev. A* **72**, 053612 (2005).
- [11] B. Damski, H. U. Everts, A. Honecker, H. Fehrmann, L. Santos, and M. Lewenstein, *Phys. Rev. Lett.* **95**, 060403 (2005).
- [12] J. Ruostekoski, *Phys. Rev. Lett.* **103**, 080406 (2009).
- [13] M. Greiner, O. Mandel, T. Esslinger, T. W. Hänsch, and I. Bloch, *Nature (London)* **415**, 39 (2002).
- [14] D. Hellweg, L. Cacciapuoti, M. Kottke, T. Schulte, K. Sengstock, W. Ertmer, and J. J. Arlt, *Phys. Rev. Lett.* **91**, 010406 (2003).
- [15] Y. Shin, C. H. Schunck, A. Schirotzek, and W. Ketterle, *Nature (London)* **451**, 689 (2008).
- [16] R. Jördans, N. Strohmaier, K. Günter, H. Moritz, and T. Esslinger, *Nature (London)* **455**, 204 (2008).
- [17] N. Gemelke, X. Zhang, C. L. Hung, and C. Chin, *Nature (London)* **460**, 995 (2009).
- [18] R. Jördens, L. Tarruell, D. Greif, T. Uehlinger, N. Strohmaier, H. Moritz, T. Esslinger, L. De Leo, C. Kollath, A. Georges, V. Scarola, L. Pollet, E. Burovski, E. Kozik, and M. Troyer, *Phys. Rev. Lett.* **104**, 180401 (2010).
- [19] U. Schneider, L. Hackermüller, S. Will, Th. Best, I. Bloch,

- T. A. Costi, R. W. Helmes, D. Rasch, and A. Rosch, *Science* **322**, 1520 (2009).
- [20] T. Ohashi, T. Momoi, H. Tsunetsugu, and N. Kawakami, *Phys. Rev. Lett.* **100**, 076402 (2008).
- [21] T. Yoshioka, A. Koga, and N. Kawakami, *Phys. Rev. Lett.* **103**, 036401 (2009).
- [22] D. Galanakis, T. D. Stanescu, and P. Phillips, *Phys. Rev. B* **79**, 115116 (2009).
- [23] K. Aryanpour, W. E. Pickett, and R. T. Scalettar, *Phys. Rev. B* **74**, 085117 (2006).
- [24] S. G. Bhongale, and H. Pu, *Phys. Rev. A* **78**, 061606 (2008).
- [25] P. B. He, Q. Sun, P. Li, S. Q. Shen, and W. M. Liu, *Phys. Rev. A* **76**, 043618 (2007).
- [26] V. V. Konotop, and M. Salerno, *Phys. Rev. A* **65**, 021602 (2002).
- [27] Y. Kato, Q. Zhou, N. Kawashima, and N. Trivedi, *Nature Physics* **4**, 614 (2008).
- [28] Z. D. Li, Q. Y. Li, P. B. He, J. Q. Liang, W. M. Liu, G. S. Fu, *Phys. Rev. A* **81**, 015602 (2010).
- [29] T. Ohashi, N. Kawakami, and H. Tsunetsugu, *Phys. Rev. Lett.* **97**, 066401 (2006).
- [30] A. Georges, G. Kotliar, W. Krauth, and M. J. Rozenberg, *Rev. Mod. Phys.* **68**, 13 (1996).
- [31] W. Metzner, and D. Vollhardt, *Phys. Rev. Lett.* **62**, 324 (1989).
- [32] R. W. Helmes, T. A. Costi, and A. Rosch, *Phys. Rev. Lett.* **100**, 056403 (2008).
- [33] T. Maier, M. Jarrell, T. Pruschke, and M. H. Hettler, *Rev. Mod. Phys.* **77**, 1027 (2005).
- [34] M. Jarrell, and H. R. Krishnamurthy, *Phys. Rev. B* **63**, 125102 (2001).
- [35] Y. Imai, and N. Kawakami, *Phys. Rev. B* **65**, 233103 (2002).
- [36] H. Lee, G. Li, and H. Monien, *Phys. Rev. B* **78**, 205117 (2008).
- [37] A. N. Rubtsov, V. V. Savkin, and A. I. Lichtenstein, *Phys. Rev. B* **72**, 035122 (2005).
- [38] L. M. Duan, *Phys. Rev. Lett.* **95**, 243202 (2005).
- [39] C. Chin, R. Grimm, P. Julienne, and E. Tiesinga, *Rev. Mod. Phys.* **82**, 1225 (2010).
- [40] M. Jarrell, and J. E. Gubernatis, *Phys. Rep.* **269**, 133 (1996).
- [41] O. Parcollet, G. Biroli, and G. Kotliar, *Phys. Rev. Lett.* **92**, 226402 (2004).
- [42] K. M. O'Hara, S. L. Hemmer, M. E. Gehm, S. R. Granade, J. E. Thomas, *Science* **298**, 2179 (2002).
- [43] S. Tung, V. Schweikhard, and E. A. Cornell, *Phys. Rev. Lett.* **97**, 240402 (2006).
- [44] T. Loftus, C. A. Regal, C. Ticknor, J. L. Bohn, and D. S. Jin, *Phys. Rev. Lett.* **88**, 173201 (2002).
- [45] M. W. Zwierlein, A. Schirotzek, C. H. Schunck, W. Ketterle, *Science* **311**, 492 (2006).
- [46] C. A. Regal, C. Ticknor, J. L. Bohn, and D. S. Jin, *Nature (London)* **424**, 47 (2003).
- [47] C. Klempt, T. Henninger, O. Topic, J. Will, W. Ertmer, E. Tiemann, and J. Arlt, *Phys. Rev. A* **76**, 020701 (2007).
- [48] T. Stöferle, H. Moritz, K. Günter, M. Köhl, and T. Esslinger, *Phys. Rev. Lett.* **96**, 030401 (2006).
- [49] N. Strohmaier, Y. Takasu, K. Günter, R. Jördens, M. Köhl, H. Moritz, and T. Esslinger, *Phys. Rev. Lett.* **99**, 220601 (2007).
- [50] M. Köhl, H. Moritz, T. Stöferle, K. Günter, and T. Esslinger, *Phys. Rev. Lett.* **94**, 080403 (2005).
- [51] J. K. Chin, D. E. Miller, Y. Liu, C. Stan, W. Setiawan, C. Sanner, K. Xu, and W. Ketterle, *Nature (London)* **443**, 961 (2006).